Monthly Notices
of the
ROYAL ASTRONOMICAL SOCIETY

MNRAS **448,** 1494–1503 (2015) doi:10.1093/mnras/stv088

Far-infrared observations of an unbiased sample of gamma-ray burst host galaxies

S. A. Kohn,[1,2★] M. J. Michałowski,[1] N. Bourne,[1] M. Baes,[3] J. Fritz,[3,4] A. Cooray,[5] I. de Looze,[3,6] G. De Zotti,[7,8] H. Dannerbauer,[9] L. Dunne,[1,10] S. Dye,[11] S. Eales,[12] C. Furlanetto,[11] J. Gonzalez-Nuevo,[13,7] E. Ibar,[14] R. J. Ivison,[1,15] S. J. Maddox,[1,10] D. Scott,[16] D. J. B. Smith,[17] M. W. L. Smith,[12] M. Symeonidis[18,19] and E. Valiante[12]

[1]*Institute for Astronomy, University of Edinburgh, Royal Observatory, Blackford Hill, Edinburgh EH9 3HJ, UK*
[2]*Department of Physics and Astronomy, University of Pennsylvania, Philadelphia, PA 19104, USA*
[3]*Sterrenkundig Observatorium, Universiteit Gent, Krijgslaan 281 S9, B-9000 Gent, Belgium*
[4]*Centro de Radioastronomía y Astrofísica, CRyA, UNAM, Campus Morelia, A.P. 3-72, C.P. 58089 Michoacán, Mexico*
[5]*Center for Cosmology, Department of Physics and Astronomy, University of California, Irvine, CA 92697, USA*
[6]*Institute of Astronomy, University of Cambridge, Madingley Road, Cambridge CB3 0HA, UK*
[7]*SISSA, Via Bonomea 265, I-34136 Trieste, Italy*
[8]*INAF-Osservatorio Astronomico di Padova, Vicolo dell'Osservatorio 5, I-35122 Padova, Italy*
[9]*Institut für Astrophysik, Universität Wien, Türkenschanzstraße 17, 1180 Wien, Austria*
[10]*University of Canterbury, Department of Physics and Astronomy, Private Bag 4800, Christchurch, 8041, New Zealand*
[11]*School of Physics & Astronomy, University of Nottingham, University Park, Nottingham NG7 2RD, UK*
[12]*Cardiff School of Physics and Astronomy Cardiff University, Queen's Buildings, The Parade, Cardiff CF24 3AA, UK*
[13]*Inst. de Fisica de Cantabria (CSIC-UC), Avda. los Castros s/n, E-39005 Santander, Spain*
[14]*Instituto de Física y Astronomía, Universidad de Valparaíso, Avda. Gran Bretaña 1111, Valparaíso, 5030 Chile*
[15]*European Southern Observatory, Karl Schwarzschild Strasse 2, D-85748 Garching, Germany*
[16]*Department of Physics & Astronomy, University of British Columbia, Vancouver, BC V6T 1Z1 Canada*
[17]*Centre for Astrophysics, Science & Technology Research Institute, University of Hertfordshire, Hatfield, Herts AL10 9AB, UK*
[18]*Astronomy Centre, Department of Physics & Astronomy, University of Sussex, Brighton BN1 9QH, UK*
[19]*Mullard Space Science Laboratory, University College London, Holmbury St Mary, Dorking, Surrey RH5 6NT, UK*

Accepted 2015 January 14. Received 2015 January 13; in original form 2014 November 5

ABSTRACT

Gamma-ray bursts (GRBs) are the most energetic phenomena in the Universe; believed to result from the collapse and subsequent explosion of massive stars. Even though it has profound consequences for our understanding of their nature and selection biases, little is known about the dust properties of the galaxies hosting GRBs. We present analysis of the far-infrared properties of an unbiased sample of 20 *BeppoSAX* and *Swift* GRB host galaxies (at an average redshift of $z = 3.1$) located in the *Herschel* Astrophysical Terahertz Large Area Survey, the *Herschel* Virgo Cluster Survey, the *Herschel* Fornax Cluster Survey, the *Herschel* Stripe 82 Survey and the *Herschel* Multi-tiered Extragalactic Survey, totalling 880 deg^2, or ∼3 per cent of the sky in total. Our sample selection is serendipitous, based only on whether the X-ray position of a GRB lies within a large-scale *Herschel* survey – therefore our sample can be considered completely unbiased. Using deep data at wavelengths of 100–500 μm, we tentatively detected 1 out of 20 GRB hosts located in these fields. We constrain their dust masses and star formation rates (SFRs), and discuss these in the context of recent measurements of submillimetre galaxies and ultraluminous infrared galaxies. The average far-infrared flux of our sample gives an upper limit on SFR of $<114\ \mathrm{M_\odot\ yr^{-1}}$. The detection rate of GRB hosts is consistent with that predicted assuming that GRBs trace the cosmic SFR density in an unbiased way, i.e. that the fraction of GRB hosts with SFR $> 500\ \mathrm{M_\odot\ yr^{-1}}$ is consistent with the contribution of such luminous galaxies to the cosmic star formation density.

Key words: gamma-ray burst: general – dust, extinction – galaxies: high-redshift – galaxies: star formation – infrared: galaxies.

★ E-mail: saulkohn@sas.upenn.edu

1 INTRODUCTION

Long-duration gamma-ray bursts (GRBs) have, in many cases, been proven to be connected with supernovae (e.g. Galama et al. 1998; Hjorth et al. 2003), suggesting that their progenitor stars are short lived (Heger et al. 2003). As a result, GRBs are expected to be located in regions undergoing active star formation, making GRBs potentially ideal tracers of star formation across a large range of redshifts and helping us to chart the star-forming history of our Universe (e.g. Wijers et al. 1998; Yonetoku et al. 2004).

Many properties of GRBs are useful for accomplishing the above task. Their extremely high luminosity at gamma-ray wavelengths allows for their detection out to very high redshift, with minimal extinction from gas or dust. The average GRB redshift is $z \sim 2.2$ (Jakobsson et al. 2006, 2012; Fynbo et al. 2009; Hjorth et al. 2012), but in principle GRBs should be visible out to $z \geq 15$–20 (Lamb & Reichart 2000), and in practice they have been observed out to $z \sim 9$ (Salvaterra et al. 2009; Tanvir et al. 2009; Cucchiara et al. 2011). Moreover, detections of GRBs are independent of the luminosity of their host galaxies, which allows us to probe fainter galaxies than in typical flux-limited samples (e.g. Tanvir et al. 2012). Previous studies have found that GRB hosts are mostly faint and blue (Le Floc'h et al. 2003), with the GRB occurring in (rest-frame) UV-bright regions (Bloom, Kulkarni & Djorgovski 2002; Fruchter et al. 2006; Leloudas et al. 2010, 2011), which is consistent with active star formation. More recent studies (e.g. Greiner et al. 2011; Krühler et al. 2011; Rossi et al. 2012; Perley et al. 2013) show that GRB hosts span a wider range of properties, suggesting that previous optically-selected host surveys were biased towards these faint blue hosts.

Before we can use GRBs to quantitatively trace star formation across cosmic history, such biases of GRB and GRB host galaxy samples must be well understood. Using The Optically Unbiased GRB Host survey (Hjorth et al. 2012), Michałowski et al. (2012) and Perley et al. (2014) analysed the radio-derived star formation rates (SFRs) of GRB hosts at $z < 2$. They found that the distributions of SFRs of GRB hosts were consistent with that of other star-forming galaxies at $z < 2$, suggesting that GRBs may be able to trace cosmic star formation; however, they made clear that further study of potential biases in the morphology and metallicity of GRB hosts is required. Similarly, Hunt et al. (2014) and Schady et al. (2014) concluded that SFRs in GRB hosts are consistent with other star-forming galaxies, and found no strong evidence for GRB hosts being biased tracers of the global star formation rate density (SFRD). However, their sample favoured infrared-bright hosts. In their study of the hosts of dust-obscured GRBs, Perley et al. (2013, 2014) found that they are not massive enough to bring the overall GRB host population into the expected territory of an unbiased SFR-tracing population for $z \sim 1$. They found that GRB hosts appear to be biased towards low-mass galaxies and suggested that the GRB rate relative to SFR is highly dependent on host-galaxy environment at this redshift, and highlighted that further studies of metallicity are needed. These findings are corroborated by Boissier et al. (2013).

Here, we attempt to study the distribution of SFRs of GRB hosts using the unbiased sample of GRBs that are located inside wide-area *Herschel*[1] (Pilbratt et al. 2010) surveys. It is important to study this aspect at both ultraviolet/optical and infrared wavelength, since these give access to unobscured and dust-obscured star formation activity, respectively. The latter is still poorly understood for GRB hosts, where deep observations and detections have been largely limited to low-redshifts and biased samples (Frail et al. 2002; Berger et al. 2003; Tanvir et al. 2004; de Ugarte Postigo et al. 2012; Wang, Chen & Huang 2012; Hatsukade et al. 2014; Hunt et al. 2014; Michałowski et al. 2014; Schady et al. 2014; Symeonidis et al. 2014). The objectives of this paper are to (1) measure the dust-obscured SFRs and dust masses of GRB host galaxies using an unbiased sample; and (2) test whether or not GRBs are unbiased tracers of cosmic star formation at $z > 2$.

The layout of this paper is as follows. Section 2 contains an overview of the *Herschel* surveys whose data we used to acquire our sample. We then discuss the measured properties of the GRB hosts in Section 3, before moving on to a more extensive discussion of these properties as compared to recent analyses of other galaxy types in Section 4. We provide out conclusions in Section 5.

We use a cosmological model of $H_0 = 70\,\mathrm{km\,s^{-1}\,Mpc^{-1}}$, $\Omega_\Lambda = 0.7$ and $\Omega_\mathrm{m} = 0.3$ and a Salpeter (Salpeter 1955) initial mass function.

2 SAMPLE AND DATA

The *Herschel* Astrophysical Terahertz Large Area Survey (H-ATLAS; Eales et al. 2010) is the largest open-time survey conducted by the *Herschel Space Observatory*. It covers approximately 600 deg^2 in the far-infrared (FIR) and submillimetre wavelengths, using PACS (100, 160 μm; Poglitsch et al. 2010) and SPIRE (250, 350 and 500 μm; Griffin et al. 2010). The *Herschel* Virgo Cluster Survey (HeViCS; Davies et al. 2010) used PACS and SPIRE to survey a total area of 84 deg^2 (Auld et al. 2013; Baes et al. 2014) of the Virgo galaxy cluster, with diminishing sensitivities beyond the central 55 deg^2. Similarly, the *Herschel* Fornax Cluster Survey (HeFoCS; Davies et al. 2013) used PACS and SPIRE to survey a total area of 16 deg^2 in the Fornax cluster. The *Herschel* Stripe 82 Survey (HerS; Viero et al. 2014) covered 79 deg^2 along the Sloan Digital Sky Survey (SDSS; York et al. 2000) 'Stripe 82' field using SPIRE. The *Herschel* Multi-tiered Extragalactic Survey (HerMES; Roseboom et al. 2010; Oliver et al. 2012; Smith et al. 2012; Viero

Table 1. Details of *Herschel* surveys used.

Survey	Area (deg^2)	Total noise (mJy beam^{-1})[a] 100	160	250	350	500	Ref.
H-ATLAS	600	25	30	7.2	8.1	8.8	1, 2
HeFoCS	16	9.9	9.2	8.9	9.4	10.2	3
HerMES[b]	100	–	–	6.4	6.8	7.6	4
HerS[c]	79	–	–	10.7	10.3	12.3	5
HeViCS	84	23	13	6.6	7.3	8.0	6

Notes. [a]The wavelength in microns of each band is given in the header.
[b]HerMES data have different noise levels depending upon the field surveyed. The average noise levels for each band are presented here, given in reference (4).
[c]Coverage of the HerS maps is not uniform. The average noise levels are presented here for the deeper part of the survey (where GRB 060908 is located, see Table 2 and reference 5).
Hyphens indicate that data were not taken or not available in that band.
References: (1) Ibar et al. (2010); (2) Pascale et al. (2011); (3) Fuller et al. (2014); (4) Smith et al. (2012); (5) Viero et al. (2014) and (6) Auld et al. (2013).

[1] *Herschel* is an *ESA Space Observatory* with science instruments provided by European-led Principal Investigator consortia and with important participation from NASA.

Table 2. GRB sample.

GRB	α (J2000)	δ (J2000)	90 per cent error (arcsec)	*Herschel* field	z	Reference
990308	185.797 6667	6.734 7500	0.3	HeViCS		Schaefer et al. (1999)
050412	181.105 3333	− 1.200 1667	3.7	GAMA12		Hjorth et al. (2012)
050522	200.144 0417	24.789 0833	3.8	NGP		Butler (2007)
051001	350.953 0417	− 31.523 1389	1.5	SGP	2.4296	Butler (2007); Hjorth et al. (2012)
060206	202.931 2917	35.050 7778	0.8	NGP	4.048	Butler (2007); Fynbo et al. (2009)
060908	31.826 7500	0.342 277 78	1.4	HerS	1.884	Hjorth et al. (2012); Jakobsson et al. (2012)
070611	1.992 416 67	− 29.755 4722	1.8	SGP	2.0394	Butler (2007); Hjorth et al. (2012)
070810A	189.963 5000	10.750 8889	1.4	HeViCS	2.17	Hjorth et al. (2012); Schady et al. (2012)
070911	25.809 5417	− 33.484 1389	3.1	SGP		Butler (2007)
071028B	354.161 7917	− 31.620 3611	0.3	SGP		Clemens et al. (2011)
080310	220.057 5000	− 0.174 8889	0.6	GAMA15	2.42	Littlejohns et al. (2012); Fox et al. (2008)
091130B	203.148 1250	34.088 5278	0.6	NGP		Butler (2007)
110128A	193.896 2917	28.065 4444	0.4	NGP	2.339	Butler (2007); Sparre et al. (2011)
110407A	186.031 3917	15.711 8417	1.0	HeViCS		Chuang et al. (2011)
111204A	336.628 3750	− 31.374 8056	1.9	SGP		Sonbas et al. (2011)
120703A	339.356 7083	− 29.723 2500	0.5	SGP		Xu et al. (2012)
120927A	136.613 7500	0.416 1944	1.4	GAMA09		Beardmore et al. (2012)
121211A	195.533 2917	30.148 5000	0.5	NGP		Chester & Mangano (2012)
130502A	138.568 9583	− 0.123 3056	1.5	GAMA09		Beardmore et al. (2013)
140102A	211.919 3750	1.333 2778	0.5	GAMA15		Hagen (2014)
140515A	186.065 0000	15.104 5556	1.8	HeViCS	6.327	Butler (2007); Chornock et al. (2014)

et al. 2013; Wang et al. 2014) used SPIRE to observe 29 fields, covering ∼100 deg^2 in total.

In this study, we use H-ATLAS GAMA, NGP and SGP data (Ibar et al. 2010; Pascale et al. 2011; Rigby et al. 2011; Smith et al. 2011; Bourne et al., in preparation; Valiante et al., in preparation), all observed HeViCS fields (V1 to V4), the HeFoCS field (Davies et al. 2013), HerS maps[2] and the second major HerMES data release[3] (Smith et al. 2012). It is important to note that each of these surveys used different numbers of cross-scans with the instruments aboard *Herschel*, resulting in different levels of sensitivity. These differences are summarized in Table 1.

Butler (2007) presented a catalogue of refined X-ray positions of *Swift*/XRT (Gehrels et al. 2004; Burrows et al. 2005) GRBs.[4] Half of the 90 per cent confidence error region radii are <2.2 arcsec. It has been shown by Fynbo et al. (2009) and Hjorth et al. (2012) that such X-ray selection, as opposed to optical selection, does not introduce any bias, as long as close to 100 per cent of the gamma-ray triggered GRBs then have good X-ray localizations obtained for them. Indeed, nearly all GRBs are detected in X-ray when prompt observations are available.

We selected all GRBs with X-ray positions (Butler 2007) inside the H-ATLAS, HeViCS and HerS fields, which amounted to 21 GRBs. GRB 990308 occurred within the HeViCS field (Schaefer et al. 1999). As this is a pre-*Swift* burst, in order to not corrupt the unbiased nature of our sample we simply provide our measurements of its flux density here, and it does not enter into any other calculations. No GRB positions overlapped with any HeFoCS or HerMES fields. The catalogue contains 780 GRBs over the entire sky, so in 880 deg^2 we expect to find $780 \times 880/41253 \simeq 17$ GRBs, which is close to the number of 20 that we found (i.e. excluding GRB 990308). Our sample selection process may be considered unbiased, since the only selection criterion applied was positional. Table 2 shows the positions and any known redshifts of the GRBs in our sample; Fig. 1 shows the *Herschel* data. For seven of our GRBs redshifts are known, and only for these cases do we provide physical properties.

3 RESULTS

We determined the FIR flux densities of GRB hosts by fitting Gaussian functions at the GRB positions in the *Herschel* maps using the respective beam sizes.[5] If a GRB host appeared to be detected at $>3\sigma$, we further investigated possible blending. We identified any obvious optical or FIR sources clearly distinct from the GRB host, and repeated the flux density measurement by fitting simultaneously two (or more) Gaussian functions at the GRB positions and at the positions of these other sources (this was performed for GRBs 060206, 070911, 071028B, 091130 and 110128A). For GRB 110128A in the deep optical image from de Ugarte Postigo et al. (2011) and Sparre et al. (2011), we found a low-z galaxy contributing to the *Herschel* flux density close to the GRB position (red circle on Fig. 1). No such obvious optical source was found close to the positions of GRB 060206 (Thoene et al. 2007), 071028B and 091130B (GAMA; Driver et al. 2009) but on the 250 μm images we identified sources that are clearly distinct from the GRB hosts.

The flux densities in each band are presented in Table 3. Noise was estimated by measuring the flux at 100 random positions around the GRB position (and in the same way as for the GRB position) and the error is the 3σ clipped mean of these measurements; it was consistent with being dominated by the confusion noise (Nguyen et al. 2010).

Only GRB 091130B was located close to a source from the H-ATLAS catalogue (9 arcsec separation, corresponding to half of the

[2] www.astro.caltech.edu/hers/

[3] hedam.lam.fr/HerMES/

[4] The catalogue (butler.lab.asu.edu//Swift/xrt_pos.html) is constantly updated. We accessed the catalogue on 2014 July 25. At this time, it had 780 entries.

[5] These were 9.4, 13.4, 18.2, 24.9 and 36.3 arcsec for the 100, 160, 250, 350 and 500 μm bands, respectively.

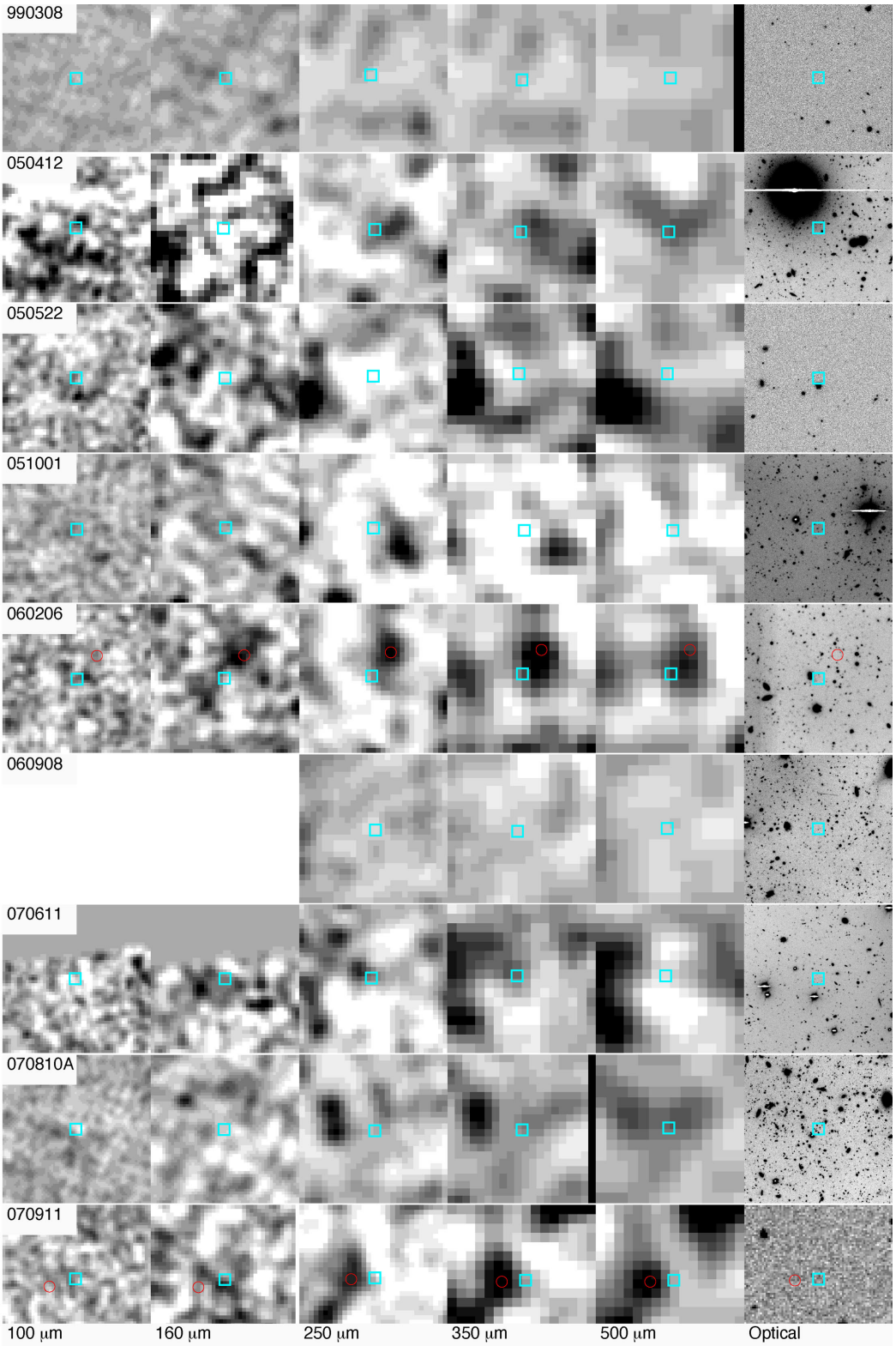

Figure 1. *Herschel* images at the positions of the GRBs in our sample. At the centre of each frame, a blue box indicates the position of the GRB, as listed in Table 2. Additional sources, which were simultaneously fitted together with the GRB positions, are marked with red circles (see Section 3). PACS images are shown from −2 (white) to 2 mJy pixel^{-1} (black). The pixel sizes are 3 and 4 arcsec for 100 and 160 μm, respectively. SPIRE images from −10 (white) to 30 mJy beam^{-1} (black). Each panel is 2 arcmin on a side. The first five columns show 100, 160 μm PACS bands, and 250, 350, 500 μm SPIRE bands, respectively, while blank frames indicate that PACS maps of these regions (HerS) are not available. The last column shows the optical data [from Hjorth et al. (2012) for 050412, 051001, 060908, 070611 and 070810A; from Thöne et al. (2008) for 060206; from de Ugarte Postigo et al. (2011) and Sparre et al. (2011) for 110128A; from SDSS (Ahn et al. 2012) for 990308, 050522 and 110407A and from GAMA (Driver et al. 2009) for 070911, 080310, 091130B, 111204A, 120703A, 120927A, 121211A, 130502A, 140102A and 140515A].

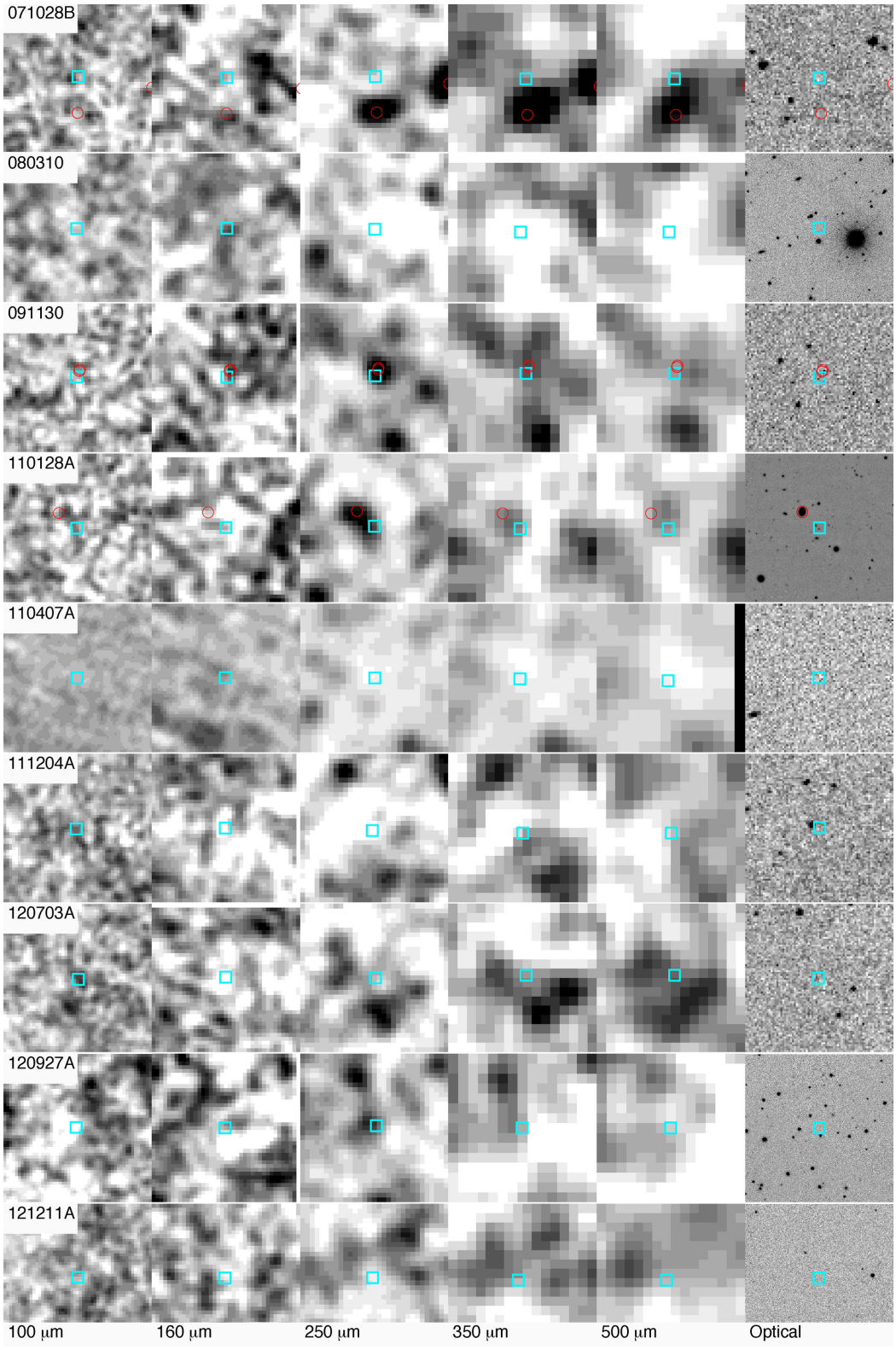

Figure 1 – *continued*

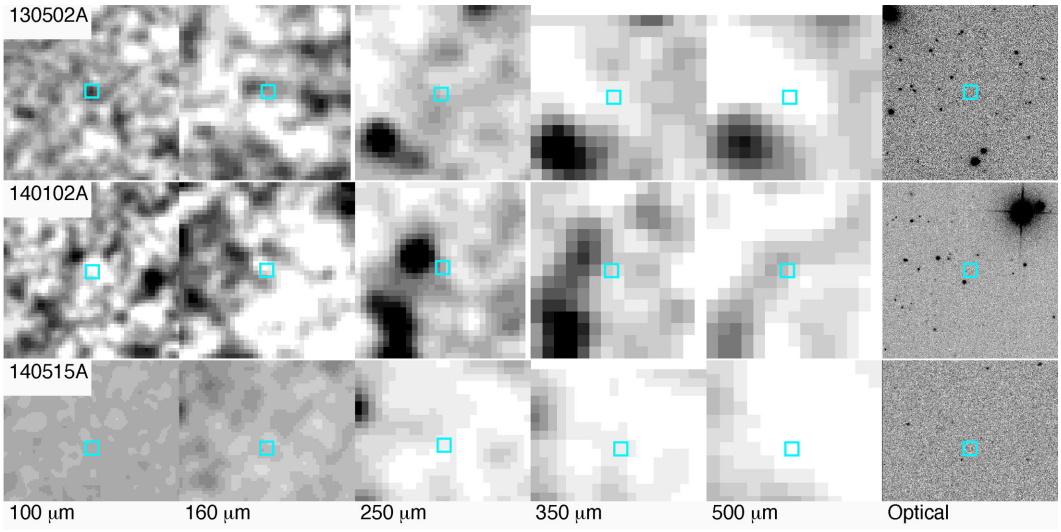

Figure 1 – *continued*

Table 3. *Herschel* flux density at GRB positions.

GRB	F100 (mJy)	F160 (mJy)	F250 (mJy)	F350 (mJy)	F500 (mJy)
990308	−13 ± 9	7 ± 12	−1 ± 7	2 ± 8	−2 ± 7
050412	−6 ± 13	−24 ± 18	7 ± 7	2 ± 8	9 ± 7
050522	12 ± 13	−17 ± 17	−10 ± 8	−7 ± 8	0 ± 9
051001	10 ± 7	3 ± 12	−5 ± 8	−4 ± 10	−6 ± 8
060206	20 ± 14	2 ± 20	8 ± 8	6 ± 11	7 ± 9
060908[a]	–	–	−8 ± 8	−3 ± 9	−2 ± 9
070611	−14 ± 20	14 ± 20	11 ± 5	12 ± 6	−3 ± 7
070810A	−30 ± 17	−19 ± 24	5 ± 10	15 ± 10	28 ± 12
070911	8 ± 11	22 ± 20	9 ± 12	3 ± 13	−7 ± 11
071028B	6 ± 14	0 ± 20	−2 ± 9	0 ± 8	3 ± 10
080310	−3 ± 11	19 ± 14	−12 ± 9	−19 ± 10	−24 ± 13
091130	−9 ± 14	−23 ± 18	−11 ± 9	4 ± 8	4 ± 8
110128A	13 ± 14	−7 ± 18	15 ± 8	6 ± 9	5 ± 9
110407A	−10 ± 11	11 ± 18	−15 ± 5	−14 ± 9	−13 ± 8
111204A	23 ± 14	−34 ± 17	−17 ± 9	−3 ± 13	5 ± 11
120703A[b]	33 ± 13	-39 ± 20	4 ± 10	0 ± 9	4 ± 11
120927A	−20 ± 13	0 ± 22	16 ± 11	−1 ± 10	−9 ± 12
121211A	−3 ± 13	−16 ± 16	−14 ± 7	−3 ± 8	−2 ± 8
130502A	22 ± 11	7 ± 14	−10 ± 5	−21 ± 8	−31 ± 9
140102A	−18 ± 12	−13 ± 17	−1 ± 8	−6 ± 9	−3 ± 8
140515A	0 ± 9	−8 ± 9	−14 ± 8	−13 ± 10	−20 ± 9
NWM[c]	2 ± 3	−4 ± 4	−3 ± 2	−2 ± 2	−3 ± 2
Stacking	1 ± 3	−2 ± 4	3 ± 2	3 ± 4	3 ± 2

Notes. Errors are from the clipped average of the flux densities of random positions around the GRB positions.
[a]GRB 060908 is inside HerS, a SPIRE-only survey.
[b]Tentative detection.
[c]Noise-weighted mean.

beam size at 250 μm). This source (HATLAS J133235.2+340526) has measured flux densities of 43 ± 6, 21 ± 7 and 7 ± 8 mJy in the 250, 350 and 500 μm bands, respectively (Rigby et al. 2011). An association between the GRB and the source is unlikely – their 9 arcsec separation is large compared to the 2 arcsec positional accuracy of the *Herschel* source.

SFRs were calculated according to Kennicutt (1998), based on the infrared luminosity integrated over 8-1000 μm using the SED of ULIRG Arp 220 (Silva et al. 1998), scaled to the flux densities of our GRB hosts. The use of Arp 220 is appropriate, since its dust temperature is close to that of typical GRB hosts (Priddey et al. 2006; Michałowski et al. 2008, 2009, 2014; Watson et al. 2011; Hatsukade et al. 2014; Hunt et al. 2014; Symeonidis et al. 2014). However, since we probe close to the peak of dust emission, the choice of the template does not influence the results substantially. For example, the median difference between the SFRs calculated using the SED of Arp 220 and the SED of a typical SMG (Michałowski, Hjorth & Watson 2010) is ∼10 per cent.

Table 4. Properties of GRBs with known redshifts.

GRB	z	Dust mass ($T = 30$ K) (10^8 $M_\odot$)	Dust mass ($T = 50$ K) (10^8 $M_\odot$)	SFR ($M_\odot$ yr^{-1})
051001	2.4296	<11	<0.9	<500
060206	4.048	<24	<2.7	<1500
060908	1.884	<6.2	<0.7	<320
070611	2.0394	5.1 ± 2.6	0.5 ± 0.2	280 ± 120
070810A	2.17	<9.8	<0.9	<520
080310	2.42	<11	<1.0	<560
110128A	2.339	<9.4	<0.9	<550
140515A	6.327	<83	<4.9	<2800
NWM[a]	2.14	<1.8	<0.3	<114
Stacking[a]	2.14	<2.4	<0.6	<114

Notes. Dust masses calculated assuming emissivity $\beta = 1.5$. Errors reflect only statistical uncertainty propagated from the flux density errors, and limits are to 2σ.
[a]These are the properties calculated from the noise-weighted mean flux density of all 21 GRB positions, at an average GRB redshift of $z = 2.14$ (Hjorth et al. 2014, Section 4).

To derive dust masses of GRB hosts, we assumed $T_{\rm dust} = 50$ K (a similar temperature to Arp 220; Klaas et al. 1997; Dunne et al. 2000; Lisenfeld, Isaak & Hills 2000; Rangwala et al. 2011), emissivity $\beta = 1.5$ (which yields conservative upper limits) and a dust absorption coefficient $\kappa_{1.2\,\rm mm} = 0.67\,{\rm cm^2\,g^{-1}}$ (Silva et al. 1998). Assuming lower $T_{\rm dust} = 30$ K results in masses larger by a factor of ∼10. Derived properties of the GRB hosts (at $T_{\rm dust} = 30$ and 50 K) with known redshift are presented in Table 4. Fig. 2 shows the spectral energy distributions of those GRBs with known redshifts, and are overlaid on the SED of Arp 220, which was used to calculate the SFR of each host.

Stacked images in the five *Herschel* bands were obtained by averaging cut-out images around the central pixel corresponding to the J2000 coordinates of each GRB host in the SPIRE and PACS images. Using PSF-filtered images in each band, a region of 15 × 15 pixels was extracted around each position, and these images were combined using a weighted mean. Each pixel in the stacked image is the weighted mean of the corresponding pixels from all the cut-outs, weighted by the inverse variance of the flux density measurement at the GRB host position. The size of the stacked images corresponds to 45, 60, 90, 120 and 180 arcsec at each of the five bands, respectively. We did not detect any significant signal at any of the stacked images (flux densities are presented in the last row of Table 3).

4 DISCUSSION

GRBs are closely linked with star formation, but they can be used as a probe of star formation only if the number of GRBs at a given redshift is proportional to the cosmic SFRD at this epoch. In such a case the distribution of SFRs of GRB hosts should reflect the contribution of galaxies to the SFRD. In particular, the fraction of hosts above some SFR threshold should be equal to the fractional contribution of such luminous galaxies to the SFRD. If the fraction of luminous GRB hosts is lower (higher) than this contribution, then we would conclude that GRBs are biased towards less (more) actively star-forming galaxies.

Integrating the $1.8 < z < 2.3$ infrared luminosity function of Magnelli et al. (2013) above $L_{\rm IR} > 5 \times 10^{12}\,{\rm L}\odot$ (SFR $> 500\,{\rm M}_\odot\,{\rm yr}^{-1}$) we infer that such galaxies contribute 8^{+6}_{-3} per cent (a 2σ range of 3–24 per cent) to the cosmic SFRD at $z \sim 2$. If GRBs trace star formation density in an unbiased way, we would expect this percentage of GRB hosts ($1.7^{+1.3}_{-0.6}$ hosts) in our sample to be detected, because *Herschel* sensitivity allows us to detect galaxies with $L_{\rm IR} > 5 \times 10^{12}{\rm L}_\odot$ (assuming the Arp 220 template at $z = 2$–2.5 scaled to the 3σ limit of 15–20 mJy).

Out of our 21 GRB hosts, we found just one tentative detection (5 ± 5 per cent), namely GRB 120703A with a significance of $\sim 2.7\sigma$, suggesting that GRBs may trace star formation density in an unbiased way, at least for redshift $2 < z < 4$ (and the expectation of 1–3 detected hosts is an upper limit, since we are assuming that GRBs in our sample with no redshift information are at similar redshifts as the other ones). This is supporting evidence for the much sought-after relationship between GRB rate and SFR (e.g. Blain & Natarajan 2000; Lloyd-Ronning, Fryer & Ramirez-Ruiz 2002; Hernquist & Springel 2003; Christensen, Hjorth & Gorosabel 2004; Yonetoku et al. 2004; Yüksel et al. 2008; Kistler et al. 2009; Elliott et al. 2012; Michałowski et al. 2012; Robertson & Ellis 2012; Hunt et al. 2014).

However, our analysis suffers from low number statistics as none of our *Herschel* flux measurements is of high significance, we consider here how our conclusions change if they are not real (0^{+4}_{-0} per cent detection rate). That would produce a $<2\sigma$ tension between the data and the expectation that GRBs trace the star formation in an unbiased way at $z \sim 2$ (i.e. 8^{+6}_{-3} per cent detection rate). This demonstrates that a FIR survey of a larger unbiased sample of GRB hosts is crucial to reach a statistically significant conclusion.

These conclusions are not uncontested. Perley et al. (2013) found a biased correspondence between the GRB host galaxy population and SFRD (at least at $z < 1.5$). In their extensive study of the hosts of *Swift*-observed GRBs, they found that GRB rate is a strong function of host-galaxy properties. In particular, GRB hosts were found to be less massive and bluer than what would be expected if the GRB rate is proportional to SFR in galaxies at $z < 1.5$ (Perley et al. 2013). We probe GRB hosts at higher redshifts, but more significant samples of GRB hosts observed in the FIR are needed to investigate this issue.

The average 2σ upper limit of the dust mass for our sample is $\log(M_{\rm dust}/{\rm M}_\odot) = 7.4 \pm 0.3$ –8.1 ± 0.2 (50–30 K). This suggests that GRB hosts are less dusty than SMGs, as Michałowski et al. (2010) found the typical SMG to contain $\log(M_{\rm dust}/{\rm M}_\odot) = 9.02 \pm 0.36$ (also see Chapman et al. 2005; Kovács et al. 2006; Laurent et al. 2006; Coppin et al. 2008; Magnelli et al. 2012; Swinbank et al. 2014). The dust masses of GRB hosts in our sample are only consistent with those of SMGs if we assume a very low temperature of 30K (e.g. Michałowski et al. 2010 found and average temperature of 35 K for SMGs). Calzetti et al. (2000) and Smith et al. (2013) found that dust emission at much lower temperatures (20–30 K) could account for a large fraction of total flux in starburst galaxies, but other studies (Priddey et al. 2006; Michałowski et al. 2008, 2009, 2014; Symeonidis et al. 2014) suggest this is an unrealistically low temperature for an infrared-bright GRB host (however none of these studies is based on an unbiased GRB sample). Moreover, high dust temperature was found to be typical among *Herschel*-selected ULIRGs at high redshifts (Symeonidis et al. 2013).

The noise-weighted average of the flux densities at all 20 GRB positions and flux densities measured in the stacked maps are shown in Table 3. At an average GRB redshift of $z = 2.14$ (Hjorth, Gall & Michałowski 2014), this corresponds to a 2σ limit of SFR $<114\,{\rm M}_\odot\,{\rm yr}^{-1}$ ($L_{\rm IR} < 2 \times 10^{12}\,{\rm L}_\odot$) using the Arp 220 template, and 2σ limits on dust masses of $M_{\rm dust} < 2 \times 10^7\,{\rm M}_\odot$ for $T_{\rm dust} = 50$ K, and $M_{\rm dust} < 2 \times 10^8\,{\rm M}_\odot$ for $T_{\rm dust} = 30$ K. Measurements of stacked images provide consistent limits on the dust mass

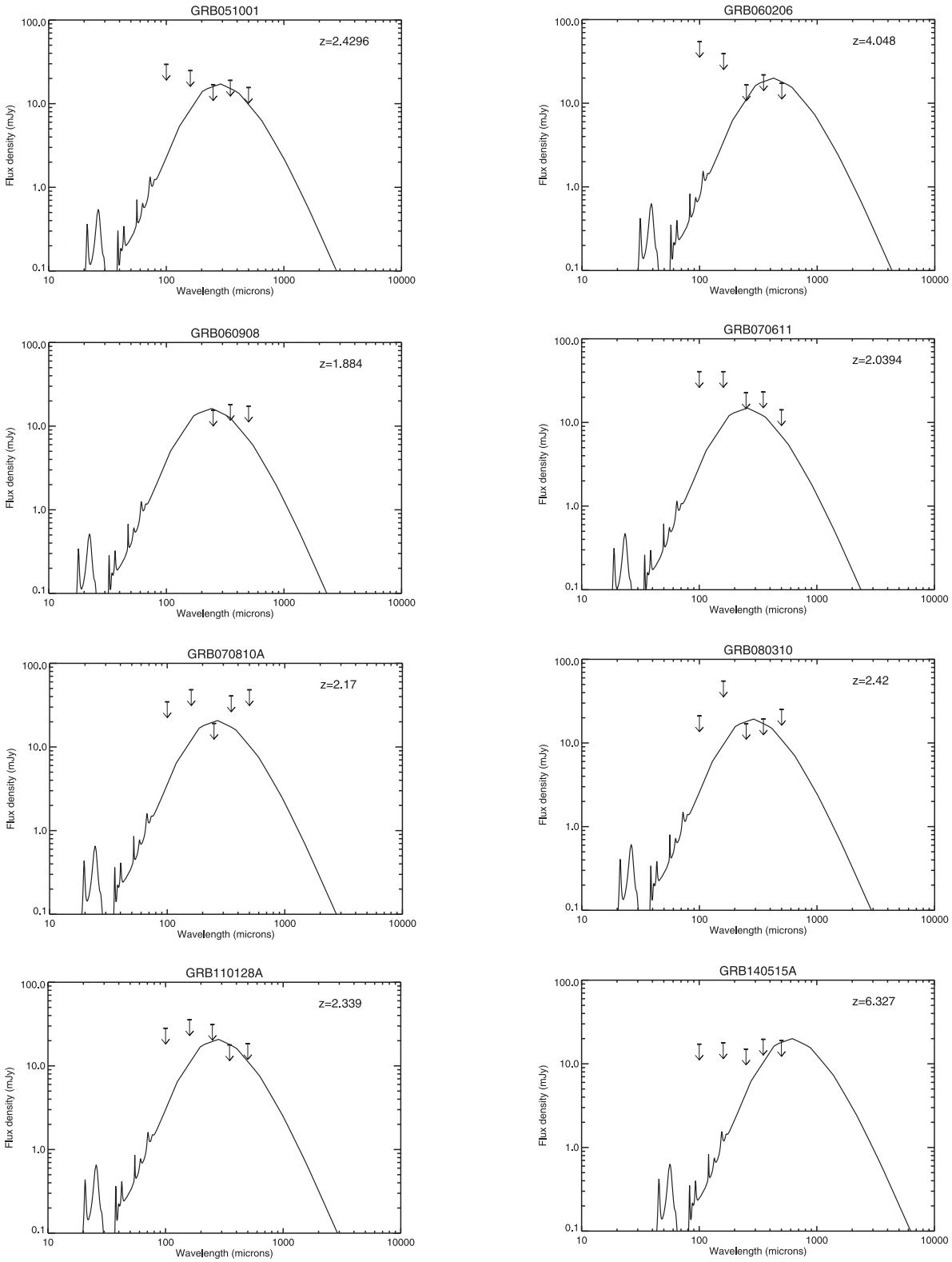

Figure 2. 2σ upper limits on the SEDs of GRBs with known redshifts overlaid with the SED of Arp 220, used to calculate the SFR of each GRB host galaxy. The SED of Arp220 has been redshifted to match each GRB, shown on the upper right of each plot. Upper limits are from the base of the arrow.

of typical GRB hosts: $M_{\rm dust} < 6 \times 10^7\,{\rm M}_\odot$ for $T_{\rm dust} = 50\,{\rm K}$, and $M_{\rm dust} < 2.4 \times 10^8\,{\rm M}_\odot$ for $T_{\rm dust} = 30\,{\rm K}$. The deepest limit on SFR comes from the stacked 250 μm band, giving a typical GRB host SFR of $<114\,{\rm M}_\odot\,{\rm yr}^{-1}$.

If GRBs trace the cosmic SFRD in an unbiased way, then the average luminosity of GRB hosts should be equal to the average luminosity of other galaxies weighted by their SFRs (because a galaxy with a higher SFR will have a higher probability to host a GRB). From the luminosity function (ϕ) of Magnelli et al. (2013), we calculated the weighted mean $\langle L\rangle_{\rm SFR} = \int_{L_{\rm min}}^{L_{\rm max}} \phi \times {\rm SFR} \times L\,{\rm d}L / \int_{L_{\rm min}}^{L_{\rm max}} \phi \times {\rm SFR}\,{\rm d}L$. Assuming ${\rm SFR} \propto L_{\rm IR}$ this gives $\langle \log(L/{\rm L}_\odot)\rangle_{\rm SFR} = 12.23 \pm 0.15$, or $\langle {\rm SFR}\rangle_{\rm SFR} = 290^{+120}_{-90}\,{\rm M}_\odot\,{\rm yr}^{-1}$ using the Kennicutt (1998) conversion and assuming the Saltpeter IMF (propagating the errors on luminosity function parameters using the Monte Carlo method). This value is only weakly dependent on the adopted cut-off luminosities, $\log(L_{\rm min}/{\rm L}_\odot) = 7$ and $\log(L_{\rm max}/{\rm L}_\odot) = 13$, as it is mostly constrained by the shape of the luminosity function close to its knee. Again, this value is only $<2\sigma$ away from the limit we measured for GRB hosts ($<114\,{\rm M}_\odot\,{\rm yr}^{-1}$), so we cannot rule out that GRB hosts are simply drawn based on the SFRs from the general population of galaxies, and we highlight that larger samples of unbiased GRB hosts observed at the FIR are needed.

The average flux density suggests that a typical GRB host has a flux below the confusion limit of *Herschel*, so surveys with better resolution are needed to detect the majority of the population. Such surveys will be undertaken in the future with the Large Millimeter Telescope and Cerro Chajnantor Atacama Telescope.

5 CONCLUSION

We have measured the FIR flux densities of 20 GRB host galaxies. The sample was selected in a novel, unbiased fashion, in which we used a data base of GRB positions to cross-reference the positions surveyed by the H-ATLAS, HeViCS, HeFoCS, HerMES and HerS data releases. For 8 out of the 20 GRBs, redshifts are available, and for these we were able to calculate or place an upper limit on the SFR and dust mass of the host galaxy. One host was (tentatively) detected, consistent with the contribution of such bright galaxies to the SFRD in the Universe at $z \sim 2$ (Magnelli et al. 2011, 2013). This may support the thesis that the GRB rate and SFR are fundamentally related, and that GRBs may trace SFRD in an unbiased way. Analysing a larger sample of GRB hosts selected in such an unbiased way is necessary to give a definite answer on whether this is indeed the case.

ACKNOWLEDGEMENTS

We thank Daniele Malesani and Christina Thöne for their contributions of additional optical data, and the anonymous referee for their helpful comments, which improved the quality of the paper. MJM acknowledges the support of the UK Science and Technology Facilities Council. NB is supported by the EC FP7 SPACE project ASTRODEEP (Ref. No. 312725). EI acknowledges funding from CONICYT/FONDECYT postdoctoral project no. 3130504. LD, RJI and SJM acknowledge support from ERC Advanced Grant COSMICISM. JGN acknowledges financial support from the Spanish CSIC for a JAE-DOC fellowship, co-funded by the European Social Fund, by the Spanish Ministerio de Ciencia e Innovacion, AYA2012-39475-C02-01, and Consolider-Ingenio 2010, CSD2010-00064, projects.

The *Herschel*-ATLAS is a project with *Herschel*, which is an *ESA Space Observatory* with science instruments provided by European-led Principal Investigator consortia and with important participation from NASA. The H-ATLAS website is http://www.h-atlas.org/.

GAMA is a joint European-Australasian project based around a spectroscopic campaign using the Anglo-Australian Telescope. The GAMA input catalogue is based on data taken from the SDSS and the UKIRT Infrared Deep Sky Survey. Complementary imaging of the GAMA regions is being obtained by a number of independent survey programmes including *GALEX* MIS, VST KIDS, VISTA, VIKING, *WISE*, *Herschel*-ATLAS, GMRT and ASKAP providing UV to radio coverage. GAMA is funded by the STFC (UK), the ARC (Australia), the AAO and the participating institutions. The GAMA website is http://www.gama-survey.org/.

This research has made use of data from HerMES project (http://hermes.sussex.ac.uk/). HerMES is a *Herschel* Key Programme utilizing Guaranteed Time from the SPIRE instrument team, ESAC scientists and a mission scientist. The HerMES data were accessed through the *Herschel* Database in Marseille (HeDaM – http://hedam.lam.fr) operated by CeSAM and hosted by the Laboratoire d'Astrophysique de Marseille.

Funding for SDSS-III has been provided by the Alfred P. Sloan Foundation, the Participating Institutions, the National Science Foundation, and the US Department of Energy Office of Science. The SDSS-III website is http://www.sdss3.org/.

REFERENCES

Ahn C. P. et al., 2012, ApJS, 203, 21
Auld R. et al., 2013, MNRAS, 428, 1880
Baes M. et al., 2014, A&A, 562, A106
Beardmore A. P., Evans P. A., Goad M. R., Osborne J. P., 2012, GCN Circ., 13824, 1
Beardmore A. P., Evans P. A., Goad M. R., Osborne J. P., 2013, GCN Circ., 14536, 1
Berger E., Cowie L. L., Kulkarni S. R., Frail D. A., Aussel H., Barger A. J., 2003, ApJ, 588, 99
Blain A. W., Natarajan P., 2000, MNRAS, 312, L35
Bloom J., Kulkarni S., Djorgovski S., 2002, ApJ, 123, 1111
Boissier S., Salvaterra R., Le Floc'h E., Basa S., Buat V., Prantzos N., Vergani S. D., Savaglio S., 2013, A&A, 557, A34
Burrows D. N. et al., 2005, Space Sci. Rev., 120, 165
Butler N., 2007, AJ, 133, 1027
Calzetti D., Armus L., Bohlin R. C., Kinney A. L., Koornneef J., Storchi-Bergmann T., 2000, ApJ, 533, 682
Chapman S. C., Blain A. W., Smail I., Ivison R. J., 2005, ApJ, 622, 772
Chester M. M., Mangano V., 2012, GCN Circ., 14063, 1
Chornock R., Berger E., Fox D. B., Fong W., Laskar T., Roth K. C., 2014, ApJL, preprint (arXiv:1405.7400)
Christensen L., Hjorth J., Gorosabel J., 2004, A&A, 425, 913
Chuang C. J., Lin C. S., Urata Y., Huang K. Y., 2011, GCN Circ., 11901, 1
Clemens C. et al., 2011, A&A, 529, A110
Coppin K. et al., 2008, MNRAS, 384, 1597
Cucchiara A. et al., 2011, ApJ, 736, 7
Davies J. I. et al., 2010, A&A, 518, L48
Davies J. I. et al., 2013, MNRAS, 428, 834
de Ugarte Postigo A., Malesani D., McCormac J., Jakobsson P., 2011, GCN Circ., 11605, 1
de Ugarte Postigo A. et al., 2012, A&A, 538, A44
Driver S. P. et al., 2009, Astron. Geophys., 50, 12
Dunne L., Eales S., Edmunds M., Ivison R., Alexander P., Clements D. L., 2000, MNRAS, 315, 115
Eales S. et al., 2010, PASP, 122, 499

Elliott J., Greiner J., Khochfar S., Schady P., Johnson J. L., Rau A., 2012, A&A, 539, A113
Fox A. J., Ledoux C., Vreeswijk P. M., Smette A., Jaunsen A. O., 2008, A&A, 491, 189
Frail D. A. et al., 2002, ApJ, 565, 829
Fruchter A. S. et al., 2006, Nature, 441, 463
Fuller C. et al., 2014, MNRAS, 440, 1571
Fynbo J. P. U. et al., 2009, ApJS, 185, 526
Galama T. J. et al., 1998, Nature, 395, 670
Gehrels N. et al., 2004, ApJ, 611, 1005
Greiner J. et al., 2011, A&A, 526, A30
Griffin M. J. et al., 2010, A&A, 518, L3
Hagen L. M. Z., 2014, GCN Circ., 15690, 1
Hatsukade B., Ohta K., Endo A., Nakanishi K., Tamura Y., Hashimoto T., Kohno K., 2014, Nature, 510, 247
Heger A., Fryer C. L., Woosley S. E., Langer N., Hartmann D. H., 2003, ApJ, 591, 288
Hernquist L., Springel V., 2003, MNRAS, 341, 1253
Hjorth J. et al., 2003, Nature, 423, 847
Hjorth J. et al., 2012, ApJ, 756, 187
Hjorth J., Gall C., Michałowski M. J., 2014, ApJ, 782, L23
Hunt L. K. et al., 2014, A&A, 565, A112
Ibar E. et al., 2010, MNRAS, 409, 38
Jakobsson P. et al., 2006, A&A, 447, 897
Jakobsson P. et al., 2012, ApJ, 752, 62
Kennicutt R. C., 1998, Annu. Rev. Astron. Astrophys., 36, 189
Kistler M. D., Yüksel H., Beacom J. F., Hopkins A. M., Wyithe J. S. B., 2009, ApJ, 705, L104
Klaas U., Haas M., Heinrichsen I., Schulz B., 1997, A&A, 325, L21
Kovács A., Chapman S. C., Dowell C. D., Blain A. W., Ivison R. J., Smail I., Phillips T. G., 2006, ApJ, 650, 592
Krühler T. et al., 2011, A&A, 534, A108
Lamb D. Q., Reichart D. E., 2000, ApJ, 536, 1
Laurent G. T. et al., 2006, ApJ, 643, 38
Le Floc'h E. et al., 2003, A&A, 400, 499
Leloudas G., Sollerman J., Levan A. J., Fynbo J. P. U., Malesani D., Maund J. R., 2010, A&A, 518, A29
Leloudas G. et al., 2011, A&A, 530, A95
Lisenfeld U., Isaak K. G., Hills R., 2000, MNRAS, 312, 433
Littlejohns O. M. et al., 2012, MNRAS, 421, 2692
Lloyd-Ronning N. M., Fryer C. L., Ramirez-Ruiz E., 2002, ApJ, 574, 554
Magnelli B., Elbaz D., Chary R. R., Dickinson M., Le Borgne D., Frayer D. T., Willmer C. N. A., 2011, A&A, 528, A35
Magnelli B. et al., 2012, A&A, 539, A155
Magnelli B. et al., 2013, A&A, 553, A132
Michałowski M. J., Hjorth J., Castro Cerón J. M., Watson D., 2008, ApJ, 672, 817
Michałowski M. J. et al., 2009, ApJ, 693, 347
Michałowski M., Hjorth J., Watson D., 2010, A&A, 514, A67
Michałowski M. J. et al., 2012, ApJ, 755, 85
Michałowski M. J. et al., 2014, A&A, 562, A70
Nguyen H. T. et al., 2010, A&A, 518, L5
Oliver S. J. et al., 2012, MNRAS, 424, 1614
Pascale E. et al., 2011, MNRAS, 415, 911
Perley D. A. et al., 2013, ApJ, 778, 128
Perley D. A. et al., 2014, ApJ, preprint (arXiv:1407.4456)
Pilbratt G. L. et al., 2010, A&A, 518, L1
Poglitsch A. et al., 2010, A&A, 518, L2
Priddey R. S., Tanvir N. R., Levan A. J., Fruchter A. S., Kouveliotou C., Smith I. A., Wijers R. A. M. J., 2006, MNRAS, 369, 1189
Rangwala N. et al., 2011, ApJ, 743, 94
Rigby E. E. et al., 2011, MNRAS, 415, 2336
Robertson B. E., Ellis R. S., 2012, ApJ, 744, 95
Roseboom I. G. et al., 2010, MNRAS, 409, 48
Rossi A. et al., 2012, A&A, 545, A77
Salpeter E. E., 1955, ApJ, 121, 161
Salvaterra R. et al., 2009, Nature, 461, 1258
Schady P. et al., 2012, A&A, 537, A15
Schady P. et al., 2014, A&A, 570, A52
Schaefer B. E. et al., 1999, ApJ, 524, L103
Silva L., Granato G. L., Bressan A., Danese L., 1998, ApJ, 509, 103
Smith D. J. B. et al., 2011, MNRAS, 416, 857
Smith A. J. et al., 2012, MNRAS, 419, 377
Smith D. J. B. et al., 2013, MNRAS, 436, 2435
Sonbas E. et al., 2011, GCN Circ., 12612, 1
Sparre M. et al., 2011, GCN Circ., 11607, 1
Swinbank A. M. et al., 2014, MNRAS, 438, 1267
Symeonidis M. et al., 2013, MNRAS, 431, 2317
Symeonidis M. et al., 2014, MNRAS, 443, L124
Tanvir N. R. et al., 2004, MNRAS, 352, 1073
Tanvir N. R. et al., 2009, Nature, 461, 1254
Tanvir N. R. et al., 2012, ApJ, 754, 46
Thoene C. C., Perley D. A., Cooke J., Bloom J. S., Chen H.-W., Barton E., 2007, GCN Circ., 6741, 1
Thöne C. C. et al., 2008, A&A, 489, 37
Viero M. P. et al., 2013, ApJ, 772, 77
Viero M. P. et al., 2014, ApJS, 210, 22
Wang W.-H., Chen H.-W., Huang K.-Y., 2012, ApJ, 761, L32
Wang L. et al., 2014, MNRAS, 444, 2870
Watson D. et al., 2011, ApJ, 741, 58
Wijers R. A. M. J., Bloom J. S., Bagla J. S., Natarajan P., 1998, MNRAS, 294, L13
Xu D., Malesani D., Fynbo J. P. U., Tanvir N. R., Karhunen K., 2012, GCN Circ., 13411, 1
Yonetoku D., Murakami T., Nakamura T., Yamazaki R., Inoue A. K., Ioka K., 2004, ApJ, 609, 935
York D. G. et al., 2000, AJ, 120, 1579
Yüksel H., Kistler M. D., Beacom J. F., Hopkins A. M., 2008, ApJ, 683, L5

This paper has been typeset from a TEX/LATEX file prepared by the author.